

**NANOCRYSTALLINE ZEOLITES AS CRACKING CATALYSTS IN THE
PRODUCTION OF BIOFUEL FROM USED PALM OIL**

by

NIKEN TAUFIQURRAHMI LISTYORINI

**Thesis submitted in fulfillment of the
requirements for the degree of
Master of Science**

January 2011

ACKNOWLEDGEMENTS

First of all, alhamdulillah, all praises to Allah the Al-Mighty for His strengths and blessings in completing my master research work. I would like to express my special appreciation to my supervisor, Professor Subhash Bhatia for his infinite perseverance, enthusiasm, patient guidance and great inspiration through the graduate program and thesis process. I really appreciate the opportunity to work under his supervision. I would like to acknowledge gratefully my co-supervisors Professor Abdul Rahman Mohamed for his helps and advices through this research work.

I would like to extend my heartiest appreciation to Ministry of Science, Technology and Innovation (MOSTI) for the allocation for funding this research through e-Science Fund grant. Not to forget, sincere thanks to all administrative staff and technicians in the school for their valuable help and co-operation. Professor Rusli Ismail from Institute Molecular Medicine (INFORMM) USM and Prof. Rosma Ahmad from School of Technology Industry USM are particularly acknowledged for permission using high speed centrifuge. I am also indebted to School of Physics, School of Biological Sciences and School of Chemical Sciences in USM for XRD, SEM, TEM and FTIR analysis.

Yin Fong, Thiam Leng, Stephanie, Fad, Kecoh, Che Mah, Kak Maria, Kak Miza, Mbak Tuti, Ipit, Nisa, Dibyo, Abot, Imam and other colleagues for your kindness, help, concern, motivation and moral supports. To those who indirectly contributed in this research, your kindness means a lot to me. Thank you very much. Last but definitely not least, my deepest and most heart-felt gratitude to my family and friends here also in Indonesia for their support, encouragement, concern and for standing by me through during this study.

Niken Taufiqurrahmi, January 2011.

TABLE OF CONTENTS

ACKNOWLEDGEMENTS	ii
TABLE OF CONTENTS	iii
LIST OF TABLES	vii
LIST OF FIGURES	ix
LIST OF SYMBOLS	xiv
LIST OF ABBREVIATIONS	xv
ABSTRAK	xvii
ABSTRACT	xix
CHAPTER 1: INTRODUCTION	
1.1 World Energy Demand	1
1.2 Alternative Fuels for Transportation	2
1.3 Biofuel	3
1.4 Catalytic Cracking	5
1.4.1 Catalytic Cracking Catalyst	6
1.5 Zeolite	6
1.6 Nanocrystalline Zeolite	8
1.7 Problem Statement	10
1.8 Objectives	11
1.9 Scope of the Study	11
1.10 Organization of the Thesis	12
CHAPTER 2: LITERATURE REVIEW	
2.1 Zeolite	15
2.1.1 Zeolite ZSM-5	18
2.1.2 Zeolite Y	20
2.1.3 Zeolite Beta	21
2.2 General Properties of Zeolite	23
2.3 Zeolite Synthesis	25
2.3.1 (a) Chemical Source	25
2.3.1 (b) Mechanism	27
2.4 Nanocrystalline Zeolite	30

2.4.1	Properties	30
2.4.2	Crystallization	32
2.4.3	Nanocrystalline Zeolite Synthesis	32
2.4.3 (a)	Synthesis from Clear Solution	33
2.4.3 (b)	Synthesis Using Growth Inhibitor	34
2.4.3 (c)	Confined Space Synthesis	35
2.4.4	Effect of Variables on the Synthesis	35
2.5	Characterization of Zeolite as Catalysts	37
2.5.1	Physical Properties	37
2.5.1 (a)	Surface Area	37
2.5.1 (b)	X-ray diffraction (XRD) Crystallography	40
2.5.1 (c)	Thermogravimetric Analysis	42
2.5.1 (d)	Fourier Transform Infra Red (FTIR)	42
2.5.1 (e)	Electron Microscopy	44
2.5.2	Chemical Properties Characterization	46
2.5.2 (a)	Acidity	46
2.6	Catalytic Cracking of Vegetable Oil	48
2.6.1	Catalytic Cracking Mechanism	51
2.7	Process Studies and Catalytic Activity	53
2.7.1	Process Modelling	53
2.7.1 (a)	Design of Experiments (DoE)	53
2.7.1 (b)	Responses Surface Methodology (RSM)	56
2.7.2	Deactivation Studies	56
2.7.3	Coke Combustion Kinetics	58
 CHAPTER 3. EXPERIMENTAL METHOD AND ANALYSIS		
3.1	Materials and Chemicals	61
3.1.1	Used Palm Oil	61
3.1.2	Chemicals and Reagents	62
3.1.3	Commercial Microcrystalline Zeolite	64
3.1.4	Overall Experimental Flowchart	65

3.2	Catalyst Preparation	66
	3.2.1 Nanocrystalline zeolite ZSM-5	66
	3.2.1(a) Preparation of 1.0M Tetrapropylammonium Hydroxide Solution	66
	3.2.1(b) Preparation Of Nanocrystalline Zeolite ZSM-5	67
	3.2.2 Nanocrystalline Zeolite Y	69
	3.2.3 Nanocrystalline Zeolite Beta	71
	3.2.4 Ion-exchange Procedure	72
3.3	Catalyst Characterization	73
	3.3.1 Nitrogen Adsorption	73
	3.3.2 X-ray Diffraction (XRD)	74
	3.3.3 Scanning Electron Microscopy (SEM)	75
	3.3.4 Transmission Electron Microscopy (TEM)	75
	3.3.5 Energy Dispersive X-ray Analysis (EDX)	76
	3.3.6 Thermal Gravimetric/ Derivative Gravimetric	76
	3.3.7 Fourier Transformed Infra Red (FTIR)	77
	3.3.8 Acidity	78
	3.3.8 (a) Fourier Transform Infra Red (FTIR) adsorbed Pyridine (PyIR)	78
	3.3.8(b) Temperature Programmed Desorption (TPD)	78
3.4	Catalyst Activity Measurement	79
	3.4.1 Fixed-bed Micro-reactor Rig	79
	3.4.1(a) Feed Section	80
	3.4.1(b) Reaction Section	81
	3.4.1(c) Product Collection Section	81
	3.4.2 Activity Test	82
	3.4.3 Products Analysis	84
	3.4.3(a) Liquid Products	84
	3.4.3(b) Gaseous Products	85
3.5	Experimental Design and Optimization	86
	3.5.1 Statistical Design of Experiments (DoE)	86
	3.5.2 Deactivation (Time on Stream) Studies	88
	3.5.3 Coke Combustion Kinetic	88

CHAPTER 4: RESULTS AND DISCUSSION	90
4.1 Zeolite Characterization	91
4.1.1 Zeolite Y	91
4.1.1 (a) Physical properties	91
4.1.1 (b) Chemical properties	99
4.1.2 Zeolite Beta	101
4.1.1 (a) Physical properties	101
4.1.1 (b) Chemical properties	109
4.1.3 Zeolite ZSM-5	111
4.1.1 (a) Physical properties	111
4.1.1 (b) Chemical Properties	118
4.1.4 Catalytic Properties of Different Zeolites	120
4.2 Catalytic Activity Studies	122
4.3 Design of Experiments (DoE) and Optimization of Process Parameters	135
4.3.1 Statistical Analysis	139
4.3.2 Process Optimization	149
4.4 Deactivation Studies	152
4.5 Coke combustion kinetics	160
4.5.1 Non-isothermal Oxidation	160
4.5.2 Isothermal Oxidation	161
4.5.2 (a) TG-DTG Characterization of the Coked Catalysts	161
4.5.2 (b) One-coke Oxidation Reaction Model	163
4.5.3 Determination of the Reaction Order n	163
 CHAPTER 5 : CONCLUSIONS AND RECOMMENDATIONS	
5.1 Conclusions	168
5.2 Recommendations	170
 REFERENCES	171
 LIST OF PUBLICATION AND CONFERENCE PRESENTATION	181

LIST OF TABLES

Table 2.1	Type of hydrocarbons produced from palm oil cracking (Iswara, 2006)	52
Table 3.1.	Composition of used palm oil and crude palm oil.	62
Table 3.2.	List of chemicals and reagents.	62
Table 3.3.	List of equipments used	63
Table 3.4.	Analytical techniques to characterize catalysts properties	73
Table 4. 1	N ₂ Adsorption desorption result of zeolite Y	96
Table 4. 2	Acid capacities of zeolite Y	100
Table 4. 3	Thermogravimetric analysis in air: weight loss (wt %) as a function of temperature	106
Table 4. 4	Nitrogen adsorption result of nanocrystalline zeolite beta	108
Table 4. 5	Acid capacities of zeolite beta	110
Table 4. 6	Nitrogen adsorption desorption result of zeolite ZSM-5	117
Table 4. 7	Acid capacities of zeolite ZSM-5	119
Table 4.8	Catalytic properties comparison	121
Table 4. 9	Catalytic cracking of UPO over microcrystalline and nanocrystallize zeolite	123
Table 4. 10	Pore size of different catalysts used	136
Table 4. 11	Independent variables range with low and high level	136
Table 4. 12	Experimental matrix and results obtained based on Design of Experiments (DoE)	137
Table 4. 13	The analysis of variance (ANOVA) for the conversion, OLP yield and gasoline yield	140
Table 4. 14	Lack of fit tests	142
Table 4. 15	Optimization criteria	150
Table 4. 16	Simulated and experimental data for conversion and gasoline fraction yield for cracking of UPO at optimum condition of nanocrystalline zeolite Y	150
Table 4. 17	Optimum condition for nanocrystalline zeolites	151

Table 4. 18	Different types of activity models proposed for different values of catalyst deactivation order, n_d .	153
Table 4. 19	The values of correlation coefficient, R^2 , activity order, n_d , activity rate constant, k_d and sum of squares, $\sum s^2$	154
Table 4. 20	Catalytic cracking of used palm oil over nanocrystalline zeolite beta with oil/catalyst ratio = 6	156
Table 4. 21	Deactivation constant (k_d) and deactivation order (n_d) at different cracking temperatures calculated from the best fitted model	159
Table 4.22	Results of the reaction order of coked nanocrystalline zeolite beta (derived at 400 °C) at various combustion temperatures, $P = 8.9$ kPa	165
Table 4.23	Activation energy from isothermal combustion of coked nanocrystalline zeolite beta at different cracking temperature	166

LIST OF FIGURES

		Page
Figure 1.1	Processes of production of Spark-Ignition engine biofuel (Demirbas, 2007)	2
Figure 1.2	3D structure of zeolite crystal a) zeolite beta (BEA), b) zeolite Linde type A (LTA), c) ZSM- 5 (MFI), d) zeolite Faujasite (FAU)	7
Figure 2.1	Zeolite basic unit structure (Guth and Kessler, 1999).	16
Figure 2.2	Schematic of Zeolite framework (Davis and Lobo, 1992)	18
Figure 2.3	Framework structure of ZSM-5 (Gates, 1992).	19
Figure 2.4	Structure of Zeolite Y (IZA, 2005)	21
Figure 2.5	Pore structure in BEA along <i>b</i> (left) and <i>a</i> (right) axis (Scherzer, 1990)	22
Figure 2.6	Brönsted and Lewis acid sites (Thanh, 2006)	23
Figure 2.7	Mechanism of zeolite crystallization (Dokter <i>et al.</i> 1995)	27
Figure 2.8	Schematic illustrations of the (A) solution-mediated transport and the(B) solution-hydrogen transformation crystallization mechanism (Davis and Lobo, 1992)	28
Figure 2.9	Proposed reaction scheme for the zeolite growth mechanism in colloidal solution (Mintova <i>et al.</i> 1999)	32
Figure 2.10	Flowchart for the preparation of nanocrystalline zeolite (Van Grieken <i>et al.</i> 2000)	34
Figure 2.11	Confined Space Synthesis mechanism Schmidt <i>et al.</i> (1999)	35
Figure 2.12	The IUPAC classification of adsorption isotherm shapes (Sing <i>et al.</i> 1985)	39
Figure 2.13	Proposed reaction pathway for the conversion of vegetable oils over zeolite cracking catalysts (Katikaneni <i>et al.</i> 1995; Leng <i>et al.</i> 1999).	50
Figure 3.1	Overall research flowchart	65
Figure 3.2	Schematic diagram of ion exchange setup (Tan, 2007)	66
Figure 3.3	Schematic diagram of hydrothermal pressure reactor	68
Figure 3.4	Flowchart for the preparation of nanocrystalline ZSM-5	69

	(Van Grieken <i>et al.</i> 2000).	
Figure 3.5	Flowchart for the preparation of nanocrystalline zeolite Y (Mintova <i>et al.</i> 1999 and Larlus <i>et al.</i> 2006).	70
Figure 3.6	Flowchart for the preparation of nanocrystalline zeolite Beta (Modhera <i>et al.</i> 2009).	72
Figure 3.7	Schematic diagram of micro-reactor rig used in catalytic cracking of used palm oil (Ooi, 2004)	80
Figure 3.8	Experimental Procedure	82
Figure 4.1	Different types of catalysts used in the cracking of UPO	90
Figure 4.2	XRD patterns of (a) nanocrystalline zeolite Y and (b) microcrystalline zeolite Y	92
Figure 4.3	SEM image of (a) microcrystalline zeolite Y (b) nanocrystalline zeolite Y	93
Figure 4.4	TEM image of nanocrystalline Zeolite Y (a) Magnification 110,000 x (b) Magnification 180,000 x	94
Figure 4.5	EDX analysis of nanocrystalline zeolite (a) Area (b) EDX analysis graphic	94
Figure 4.6	FTIR spectra of (a) nanocrystalline zeolite Y (b) microcrystalline zeolite Y	95
Figure 4.7	Nitrogen adsorption isotherm of (a) Microcrystalline zeolite Y (b) Nanocrystalline zeolite Y	97
Figure 4.8	TGA curves of (a) Microcrystalline zeolite Y (b) Nanocrystalline zeolite Y (c) As-synthesized nanocrystalline zeolite Y.	98
Figure 4.9	FTIR pyridine adsorbed spectra of (a) Microcrystalline zeolite Y (b) Nanocrystalline zeolite Y	99
Figure 4.10	NH ₃ -TPD profiles of (a) Nanocrystalline zeolite Y (b) Microcrystalline zeolite Y	101
Figure 4.11	XRD patterns of (a) Nanocrystalline zeolite beta and (b) Microcrystalline zeolite beta	102
Figure 4.12	SEM images of (a) Microcrystalline zeolite beta (b) Nanocrystalline zeolite beta	103
Figure 4.13	TEM image of nanocrystalline zeolite beta	103
Figure 4.14	EDX analysis of nanocrystalline zeolite beta (a) Area	104

	(b) EDX analysis graphic	
Figure 4.15	FTIR spectra (a) nanocrystalline zeolite beta (b) microcrystalline zeolite beta	105
Figure 4.16	TGA curves of (a) Nanocrystalline zeolite beta (b) microcrystalline zeolite beta (c) As-synthesized n- beta DTA curves of (A) Nanocrystalline zeolite beta (B) microcrystalline zeolite beta(C) As-synthesized n- beta	107
Figure 4.17	Nitrogen adsorption isotherm of (a) Microcrystalline zeolite beta(b) Nanocrystalline zeolite beta	109
Figure 4.18	Pyridine adsorbed FTIR spectra of (a) microcrystalline zeolite beta(b) nanocrystalline zeolite beta	110
Figure 4.19	NH ₃ -TPD profiles of (a) Nanocrystalline zeolite beta (b) Microcrystalline zeolite beta	111
Figure 4.20	XRD pattern of (a) Nanocrystalline zeolite ZSM-5 (b) Microcrystalline zeolite ZSM-5	112
Figure 4.21	SEM images of (a) Microcrystalline zeolite ZSM-5 (b) Nanocrystalline zeolite ZSM-5	112
Figure 4.22	TEM images of nanocrystalline zeolite ZSM-5	113
Figure 4.23	EDX analysis of nanocrystalline zeolite ZSM-5 (a) Area (b) EDX analysis graphic	114
Figure 4.24	FT-IR spectra of (a) Nanocrystalline zeolite ZSM-5	115
Figure 4.25	TGA curves of (a) Microcrystalline zeolite ZSM-5 (b) Nanocrystalline zeolite ZSM-5 (c) As-synthesized nanocrystalline zeolite ZSM-5	116
Figure 4.26	Nitrogen adsorption isotherm of (a) Microcrystalline zeolite ZSM-5 (b) Nanocrystalline zeolite ZSM-5	118
Figure 4.27	Pyridine adsorbed FTIR spectra of (a) Microcrystalline zeolite ZSM-5(b) Nanocrystalline zeolite ZSM-5	119
Figure 4.28	NH ₃ -TPD profiles of (a) Nanocrystalline zeolite ZSM-5 (b) Microcrystalline zeolite ZSM-5	120
Figure 4.29	Conversion and yield of products over different types of zeolites (Reaction temperature =450 °C , oil/cat ratio= 8, and WHSV =2.5 h ⁻¹).	127
Figure 4.30	Yield of gasoline, kerosene and diesel fractions over	129

	different types of zeolites	
Figure 4.31	Comparison of hydrocarbon product distribution obtained over different nanocrystalline zeolite	130
Figure 4.32	Effect of oil to catalyst ratio over used palm oil conversion and yield of OLP	131
Figure 4.33	Effect of reaction temperature on the conversion, OLP yield, and gasoline yield over different nanocrystalline zeolites	132
Figure 4.34	Effect of nanocrystalline zeolites structure on the distribution of aromatics present in OLP	133
Figure 4.35	Predicted versus actual conversion	144
Figure 4.36	Predicted versus actual OLP Yield	144
Figure 4.37	Predicted versus actual fraction gasoline yield	145
Figure 4.38	Three dimension response surface plot of conversion of UPO at oil/catalyst ratio = 10	146
Figure 4.39	Three dimension response surface plot of OLP yield	147
Figure 4.40	Response surface plot for gasoline fraction yield obtained from the statistical model	148
Figure 4.41	Countour plot showing the optimum gasoline fraction yield, at oil/catalyst ratio = 10.	148
Figure 4.42	Time on stream for the cracking of palm oil over different types of catalysts.	153
Figure 4.43	Conversion of used palm oil over nanocrystalline zeolite beta at different cracking temperatures and o/c ratio (6-14)	157
Figure 4.44	Experimental and predicted activity data of used palm oil cracking over different cracking temperatures against time on stream	158
Figure 4.45	Thermogravimetric curves of coked nanocrystalline zeolite beta derived at different cracking temperature with non isothermal oxidation	158
Figure 4.46	TG/DTG curves of coked nanocrystalline beta on the basis of ramped temperature experiments	162
Figure 4.47	Weight fraction of coked nanocrystalline zeolite beta	164

(derived at 400 °C) at different temperatures under the same oxygen partial pressure of 8.9 kPa

Figure 4.48 Nonlinear regression of experimental data during combustion of coked nanocrystalline zeolite beta (derived at 400 °C) at different temperature (°C) (a) 500 (b) 585

165

LIST OF SYMBOLS

NOMENCLATURES

A	Temperature code (°C)
a_0	Unit cell dimension (nm)
B	Feedstock to catalyst ratio code (g/g cat)
C	Weight hourly space velocity code (h^{-1})
E	Activation energy (kJ/mol)
F-value	Ratio of model mean square to the residuals mean square
k_d	Deactivation rate constant (h^{-1})
k_i	Reaction rate constant, $i = 1, 2, \dots, 7$ ($\text{kg}^{1-n} \text{kg}_{\text{feed}}^n \text{kg}_{\text{catalyst}}^{-1} \text{h}^{-1}$)
n	Order of reaction
n_d	Order of the deactivation rate
O/C	Oil to catalyst ratio (g/g cat)
P_c	Conversion (wt%)
R	Gas constant ($\text{J mol}^{-1} \text{K}^{-1}$)
T	Reaction temperature (°C)
t	Time on stream (h)
WHSV	Weight hourly space velocity ($\text{kg}_{\text{feed}} \text{kg}_{\text{catalyst}}^{-1} \text{h}^{-1}$)
x	Independent variable
Y	Response
Y_{product}	Yield of desired product (wt%)

Greek symbols

α	Frequency factor ($\text{kg}^{1-n} \text{kg}_{\text{feed}}^n \text{kg}_{\text{catalyst}}^{-1} \text{h}^{-1}$)
β	Constant in statistical model
ε	Error of the response Y
φ	Deactivation function
τ	Residence time (h)

LIST OF ABBREVIATIONS

a. u	Arbitrary unit
ANOVA	Analysis of variance
ASTM	American Society for Testing and Materials
BET	Brunauer-Emmett-Teller
BJH	Barrett-Joyner-Halenda
BTX	Benzene, Toluene and Xylene
CCD	Central composite design
CPO	Crude Palm Oil
CPS	Catalyst pore size
CSS	Confined space synthesis
CTABr	Hexadecyltrimethylammonium bromide
DF	Degree of freedom
DOE	Design of experiment
DTG	Derivative thermal gravimetric
EDX	Energy dispersive X-ray spectroscopy
FAU	Faujasite
FID	Flame ionization detector
FCC	Fluid Catalytic Cracking
FTIR	Fourier Transform Infrared
HRTEM	High resolution transmission electron microscopy
GC-MS	Gas Chromatography-Mass Spectrometry
ICP	Inductive Coupled Plasma
IEA	International energy association
ISO	International standard organization

IUPAC	International Union of Pure and Applied Chemistry
IZA	International Zeolite Association
LTA	Linde type A
MPOB	Malaysian Palm Oil Board
MS	Mean square
OLP	Organic liquid product
OTC	Oil to Catalyst Ratio
PSD	Pore Size Distribution
RSM	Response Surface Methodology
SEM	Scanning Electron Microscope
SS	Sum of square
TCD	Thermal Conductivity Detector
TEM	Transmission Electron Microscope
TEOS	Tetraethylorthosilicate
TEAOH	Tetra-ethyl ammonium hydroxide
TG	Thermal Gravimetric
TGA	Thermal Gravimetric Analysis
TMAOH	Tetra-methyl ammonium hydroxide
TPABr	Tetra-propyl ammonium bromide
TPD	Temperature programmed desorption
TOS	Time on Stream
UPO	Used Palm Oil
WHSV	Weight Hourly Space Velocity
XRD	X-ray diffraction
ZSM	Zeolite Socony Mobil

ZEOLIT BERKRISTAL NANO SEBAGAI MANGKIN PERETAKAN UNTUK PENGHASILAN BAHAN API BIO DARIPADA MINYAK KELAPA SAWIT TERPAKAI

ABSTRAK

Zeolit berkrystal nano dengan saiz kristal yang lebih kecil daripada 100 nm merupakan bahan yang berpotensi menggantikan mangkin zeolit yang ada disebabkan luas permukaan yang lebih besar dan batas resapan yang rendah. Nanokristalin zeolit ZSM-5 (MFI), nanokristalin zeolit Y (FAU) dan nanokristalin zeolit beta (BEA) dengan kaedah hidroterma disediakan dalam kajian ini. Zeolit yang telah disintesis telah dicirikan menggunakan belauan sinar-X (XRD), analisis permukaan (penyerapan-penyahserapan N₂), mikroskopi elektron imbasan (SEM), mikroskopi elektron transmisi (TEM), dan penyahjerapan pengaturcara suhu ammonia (TPD). Keputusan XRD zeolit nanokristal dengan pantulan yang diperluas dan puncak intensiti yang lebih rendah dengan menunjukkan adanya kristal kecil. Kristal zeolit di dalam julat 50-100 nm telah dikesan daripada analisis SEM. Saiz nano kristal zeolit telah menghasilkan luas permukaan yang besar.

Proses retakan bermangkin daripada minyak kelapa sawit terpakai untuk menghasilkan bahan api bio telah dikaji pada tekanan atmosfera dalam reaktor mikro lapisan tetap, pada suhu tindakbalas 450 °C dan halaju ruang (WHSV) pada 2.5jam⁻¹. Aktiviti zeolit nanokristalin telah dibandingkan dengan aktiviti zeolit mikrokristalin untuk mengkaji pengaruh saiz kristal.

Nanokristalin menunjukkan aktiviti yang lebih baik dalam hal penukaran minyak kelapa sawit terpakai (84 - 90 wt%), hasil produk cecair organik (OLP) (51-53% berat) dan hasil pecahan gasolin (30 - 36% berat) telah dibandingkan dengan mikrokristalin zeolit dengan penukaran minyak (71 -88% wt), hasil produk cecair organik (41-52% berat) dan hasil pecahan gasolin (16 - 35% wt). Peningkatan luas permukaan dan

kebolehcapaian bahan tindak balas memperbaiki aktiviti pemangkinan dan kememilihan produk yang dikehendaki.

Rekabentuk ujikaji (DOE) telah digunakan untuk menilai parameter proses seperti kesan suhu, nisbah minyak sawit terhadap mangkin dan saiz liang mangkin terhadap penukaran minyak kelapa sawit terpakai dan penghasilan produk yang berguna. Penghasilan OLP dan pecahan gasolin telah dapat dimaksimumkan dengan mengenal pasti keadaan optimum menggunakan kaedah sambutan permukaan. Keadaan tindakbalas optimum diperolehi pada suhu 458 °C dan nisbah minyak kelapa sawit terhadap mangkin 6.0 g.g⁻¹ memberikan hasil OLP maksimum (48.0 % berat) dan hasil pecahan gasolin (34.96 % berat) dengan zeolit nanokristal Y. Hasil optimum pecahan gasolin 37.05 (% berat) diperolehi pada suhu tindakbalas 455 °C, dan zeolite nano kristal ZSM-5 yang mempunyai nisbah mangkin kepada minyak 6.22 g.g⁻¹ memberikan penukaran 92.29 % berat. Zeolit nanokristal beta menunjukkan hasil optimum pecahan gasolin 33.61 (% berat) pada suhu tindak balas 463 °C, dan nisbah mangkin kepada minyak 7.0 g.g⁻¹ memberikan penukaran 88.17 % berat.

Kesan masa ketika aliran terhadap aktiviti telah dikaji dengan memperoleh data masa ketika aliran dengan nisbah minyak terhadap mangkin di dalam julat 6 ke 14. Perilaku pembakaran zeolit nanokristal beta yang terkok yang dihasilkan pada pelbagai suhu pengekokan dikaji dengan analisis termogravimetri (TGA). Keputusan TGA menunjukkan adanya dua jenis kok iaitu, (a) kok ringan yang boleh dihapuskan pada suhu di bawah 550 °C dan (b) kok berat, yang boleh dihapuskan pada suhu 585 °C ke atas. Tenaga pengaktifan pembakaran kok ringan adalah 118 kJ/mol berbanding dengan tenaga pengaktifan kok berat antara 157 kJ/mol. Data penyahaktifan juga dianalisis dengan menggunakan model aktiviti dan parameter penyahaktifan ditentukan.

NANOCRYSTALLINE ZEOLITE AS CRACKING CATALYSTS IN THE PRODUCTION OF BIOFUEL FROM USED PALM OIL

ABSTRACT

Nanocrystalline zeolites with a crystal size smaller than 100 nm are the potential materials replacing the existing zeolite catalysts due to their larger surface area and less diffusion limitations. Nanocrystalline zeolite ZSM-5 (MFI), nanocrystalline zeolite Y (FAU) and nanocrystalline zeolite beta (BEA) were synthesized in the present study under hydrothermal conditions. The synthesized zeolites were characterized by X-ray diffraction (XRD), Surface analysis (adsorption-desorption Nitrogen), Scanning Electron Microscopy (SEM), Transmission Electron Microscopy (TEM), and Temperature-Programmed Desorption (TPD) of ammonia. Nanocrystalline zeolites show in their XRD results, broadening of the reflections and shorter peak intensity indicating the presence of small crystals. The zeolite crystal size was in range 50-100 nm as observed from SEM. The nano size of zeolite crystals resulted in large surface area.

The cracking of used palm oil for the production of biofuel at atmospheric pressure in a fixed bed micro-reactor at reaction temperature of 450-500 °C and weight hourly space velocity (WHSV) of 2.5 h⁻¹ was studied. The activity of the nanocrystalline zeolite was compared with the activity of microcrystalline zeolite in order to study the effect of crystal size.

Nanocrystalline zeolites gave better performance in terms of used palm oil conversion (84 – 90 wt%), yield of organic liquid product (OLP) (51-53 wt %) and gasoline fraction yield (30- 36 wt %) as compare to microcrystalline zeolite with oil conversion (71 -88 wt %), OLP yield (41-52 wt %) and gasoline fraction yield (16- 35

wt %). The increase in surface area and improved accessibility of the reactant enhanced the catalytic activity and the desired product selectivity.

Design of Experiments (DoE) was used to assess the effects of process parameters such as reaction temperature, oil to catalyst ratio and catalyst pore size on the conversion of used palm oil and yield of desired products. The yield of organic liquid product (OLP) and gasoline fraction yield were maximized by determining the optimum condition using response surface methodology. The optimum reaction temperature of 458 °C and oil to catalyst ratio 6.0 gave maximum yield of OLP (48.0 wt %) and gasoline fraction yield (34.96 wt %) over nanocrystalline zeolite Y. The optimum yield of gasoline fraction of 37.05 wt % at the temperature of 455 °C and oil/catalyst ratio 6.22 with an oil conversion of 92.29 wt % was obtained over nanocrystalline zeolite ZSM-5. Nanocrystalline zeolite beta catalyst, gave the optimum yield of gasoline fraction as 33.61 wt % at a temperature 463 °C with oil/catalyst ratio 7.0 and oil conversion of 88.17 wt %.

The effect of time on stream on the catalytic activity of nanocrystalline zeolite was studied by varying the oil to catalyst ratio of 6 to 14. The combustion behavior of the coked nanocrystalline zeolite beta derived at various coking temperature of oil cracking was studied by thermogravimetric analysis (TGA). TGA results showed the presence of two types of coke namely, (a) light coke could be removed below 550°C and (b) heavy coke, which could be removed at temperature above 585°C. The activation energy of light coke combustion was 118 kJ/mol as compare to the activation energy of heavy coke about 157 kJ/mol. The deactivation data were also analyzed using activity models and the deactivation parameters were determined.

CHAPTER 1

INTRODUCTION

1.1 World Energy Demand

The world's energy supply and demand system is facing a diverse and broad set of challenges. The demand for energy is increasing continuously, because of the progress in industrialization and population increase. On the other hand, petroleum as the major fuel worldwide is limited and cannot be generated due to its finite resources (Kulkarni and Dalai, 2006). With the world total consumption of petroleum reaching 84 million barrels per day in 2005, the known petroleum reserves are estimated to be depleted in less than 50 years at the present rate of consumption by 2.7 % per year (EIA oil depletion 2002). Increasing air pollution is also one of the most important issues. Exhaust emissions from motor vehicles is the main contributor in this pollution. Apart from these emissions, petroleum fuel is also major source of other air contaminants including CO₂, NO_x, SO_x, CO, particulate matter, and volatile organic compounds (Kulkarni and Dalai, 2006).

Fast depleting energy reserves, greater environmental awareness, increasing in crude oil prices and increasing energy consumption has triggered interest in searching alternative sources to replace petroleum-based fuels. Therefore, research and development on alternative fuels is intensively carried out all over the world to meet the future needs of energy globally. One of the most promising alternative fuels is biofuel (Demirbas *et al.* 2009).

1.2 Alternative Fuels for Transportation

A substantial portion of the energy consumed was from oil which was mainly utilized in the transport and industrial sectors. There are two global transportation fuels. These are gasoline and diesel fuels. Gasoline is used as fuel in the petrol engine and used by most of the transportation sector. It is likely that role of biofuels produced from renewable resources such as biogasoline and biodiesel will be increasing in our energy future as solution to dampen further increase in petroleum prices and to address potential shortfalls in global petroleum supplies.

Recently, there is growing interest in bio oil and its derivatives as alternative fuels for internal combustion engines. Figure 1.1 presents different types of biofuels useful for spark ignition vehicles and their production methods. The type of liquid biofuels and routes include fermentation of sugar to bioethanol, catalytic cracking of natural oil and fats and decarboxylation and deoxygenation of vegetable oil and fatty acids mixture pyrolysis of biomass, Fischer-Tropsch liquids.

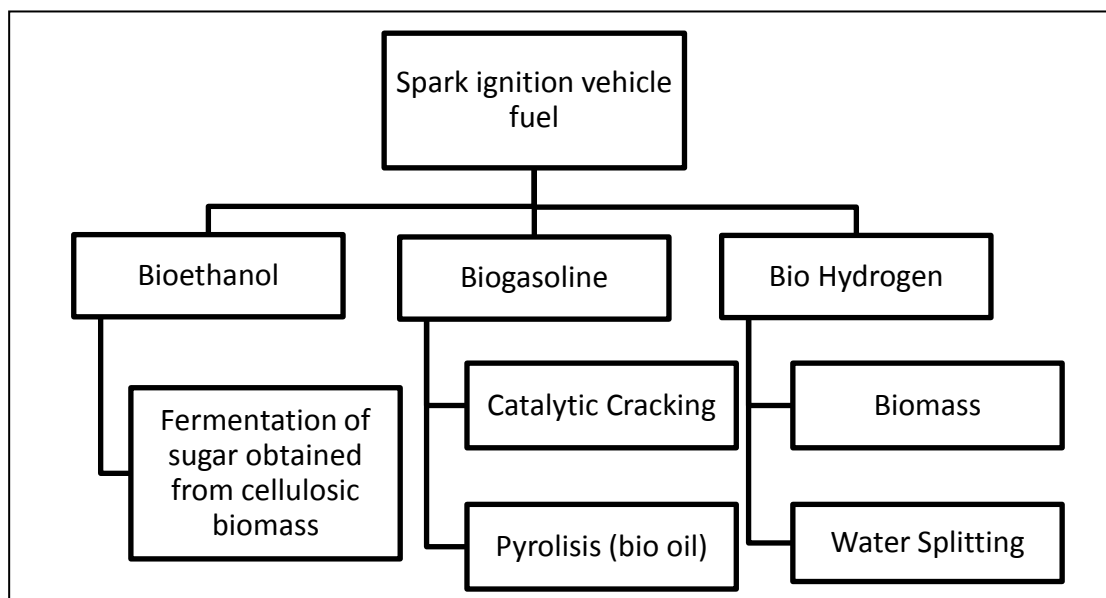


Figure. 1.1. Processes of production of Spark-Ignition engine biofuel

(Demirbas, 2007)

1.3 Biofuel

Biofuel is defined as liquid or gaseous fuel that can be produced from the utilization of biomass substrates and can serve as a (partial) substitute for fossil fuels (Giampietro *et al.* 1997). The strongest motivation for biofuel production is due to the depletion of fossil fuel, but the environmental concerns about global pollution are highlighted nowadays especially in developing countries. The production of biofuels such as diesel and gasoline fractions as an alternative fuel obtained from natural vegetables oils and fats which are environmentally friendly because they are free of nitrogen and sulfur compounds (less green house effect and less local air pollution). Biofuel can be used as fuel or fuel additive to reduce vehicle emissions (Ooi *et al.* 2004a).

Raw materials contribute to a major portion in the production of biofuel. Biomass feedstocks for biofuels include cellulosic biomass, starch-based biomass, and plant oils (Huber *et al.* 2007). Several types of plant oils, with a diversified composition in fatty acids, can be used for the preparation of bio-fuel. Plant oils are the easiest feedstock to convert into liquid fuels because of their high energy density, low oxygen content, and the fact that they are already liquid fuels. Cellulose-based biomass, which is the cheapest and most abundant form of biomass, is more difficult to convert into a biofuel because it is a solid with a low energy density. The first step for utilization of cellulosic biomass in a petroleum refinery is to overcome the recalcitrant nature of this material and convert it into a liquid product, which is done by fast pyrolysis or liquefaction to produce bio-oils or by hydrolysis routes to produce aqueous sugars and solid lignin. Catalytic cracking of bio-oils, sugars, and lignin produces olefins and aromatics from biomass-derived feedstocks (Huber *et al.* 2007).

Plant oils are those oils that are derived from plant resources. Palm oil, corn oil, soybean oil, cottonseed oil, jatropha oil, and coconut oil are all examples of plant oils. The choice of these raw materials depends mainly on its availability (Rashid *et al.* 2008), cost and climate (Barnwal and Sharma, 2005; Sharma and Singh, 2008) in each countries. In general, the most abundant vegetable oil in a particular region is the most common feedstock. In Europe, rapeseed and sunflower oils are mainly used as feedstock for biofuel production. Rapeseed or canola oil is very widely cultivated throughout the world as vegetable oil for human consumption, the production of animal food, and diesel biofuel. While in the United States, soya bean oil as one of the the most widely produced edible oil and is the major source of feedstock for manufacturing biodiesel (Biodiesel 2007). In Malaysia, oil palm is widely grown; in 2008 nearly 17.7 million tonnes of palm oil produced on 4.5 million hectares of land, and was the second largest exporter of palm oil after Indonesia (MPOB, 2010). Palm oil has been used as a raw material for oleochemical industries besides being used as cooking oil.

However, direct conversion of edible palm oil to fuels may not be economically feasible even though the results showed the potential of obtaining liquid hydrocarbons. Continuous and large-scale production of biofuel from edible oil without proper planning may cause negative impact to the world, such as depletion of food supply leading to economic imbalance (Gui *et al.* 2008). A possible solution to overcome this problem is to use non-edible oil or used edible oil. The utilization of used edible oil will not only help in cleaning up the waste but by converting them into value added chemical products. Waste cooking palm oil from restaurants and household are inexpensive compared with crude palm oil. Thus it is a promising alternative to crude palm oil for biofuel production. Reducing the cost of

the feed stocks is necessary for biofuel to be commercially viable to compete with the petroleum diesel. The consistent supply of these materials should not pose any problem in the near future. However, the desired product and the properties of biofuel from waste cooking palm oil would largely be dependent on the physicochemical properties of this feedstock (Kulkarni and Dalai, 2006).

1.4 Catalytic Cracking

Biofuel can also be produced using a direct upgrading process such as the catalytic cracking technology. The conversion of vegetable oils to fuels involves the cracking of fatty acids or tryglycerides into lighter products. The proposed reaction pathway for conversion of vegetable oils over zeolite cracking catalyst was reported by Katikaneni *et al.* (1995) and Leng *et al.* (1999).

Catalytic cracking of vegetable oils is another route to produce liquid fuels that contain linear and cyclic paraffins, olefins, aldehydes, ketones and carboxylic acids. Triglycerides, contained in vegetable oil, are easier to convert into liquid transportation fuels than cellulosic biomass because they are already high-energy liquid that contain less oxygen. Chew *et al.* (2008) reported that catalytic cracking has been extensively studied for the production of biogasoline (a potential biofuel) from palm oil. Different reaction systems have been described for studying catalytic cracking at the laboratory scale. Catalytic reactor can be classified as fixed bed, fluidized bed and entrained flow reactors. These three different types of catalytic reactors are currently employed for the laboratory evaluation of cracking catalysts (Tamunaidu, 2007).

1.4.1 Catalytic Cracking Catalyst

In the direct catalytic conversion process, the choice of catalyst controls the type of fuel and its yield in the organic liquid product. The properties of catalysts are governed by acidity, pore shape and size (Tamunaidu, 2007). Various types of zeolite catalysts are reported in the catalytic cracking for liquid fuel production from gas oil, vegetable oil, palm oil, used palm oil and palm oil based-fatty acid mixtures (Twaiq *et al.* 1999; Leng *et al.* 1999; Ooi *et al.* 2003 and 2005; Ooi and Bhatia, 2007). Zeolites have shown excellent performance as solid acid cracking catalysts due to their higher selectivity (Leng *et al.* 1999). Zeolite can be more effective for larger reactant molecules by combining their microporous structure with mesoporous materials having higher adsorption capacity (Twaiq *et al.* 2003a,b). The role of HZSM-5 in catalytic cracking unit was an octane-boosting additive due to its higher selectivity towards aromatic hydrocarbons. In addition, the primary application of Y zeolites has been in catalytic cracking of petroleum molecules into smaller gasoline range hydrocarbons.

1.5 Zeolite

Zeolites are crystalline silicates and aluminosilicates linked through oxygen atoms, producing three-dimensional network channels and cavities of molecular dimension. Structurally, the zeolite framework possesses a net negative charge which is balanced by the addition of protons (for instance, Na^+ , K^+ , or NH_4^+) due to zeolites comprise the assemblies of SiO_4 and AlO_4 tetrahedra joined together through the sharing of oxygen atoms with an open structure. Many of these cations are mobile and can readily be exchanged with other ions in a contact solution. This ion-

exchange property accounts for the greatest volume use of zeolites today. The most common method to categorize zeolites is based on their framework structure. The Structure Commission of the International Zeolite Association (IZA) identifies each framework with a three-letter mnemonic code. Figure 1.2 shows the 3-D stick structure for some of the most commonly used zeolites in the industries and their three-letter code.

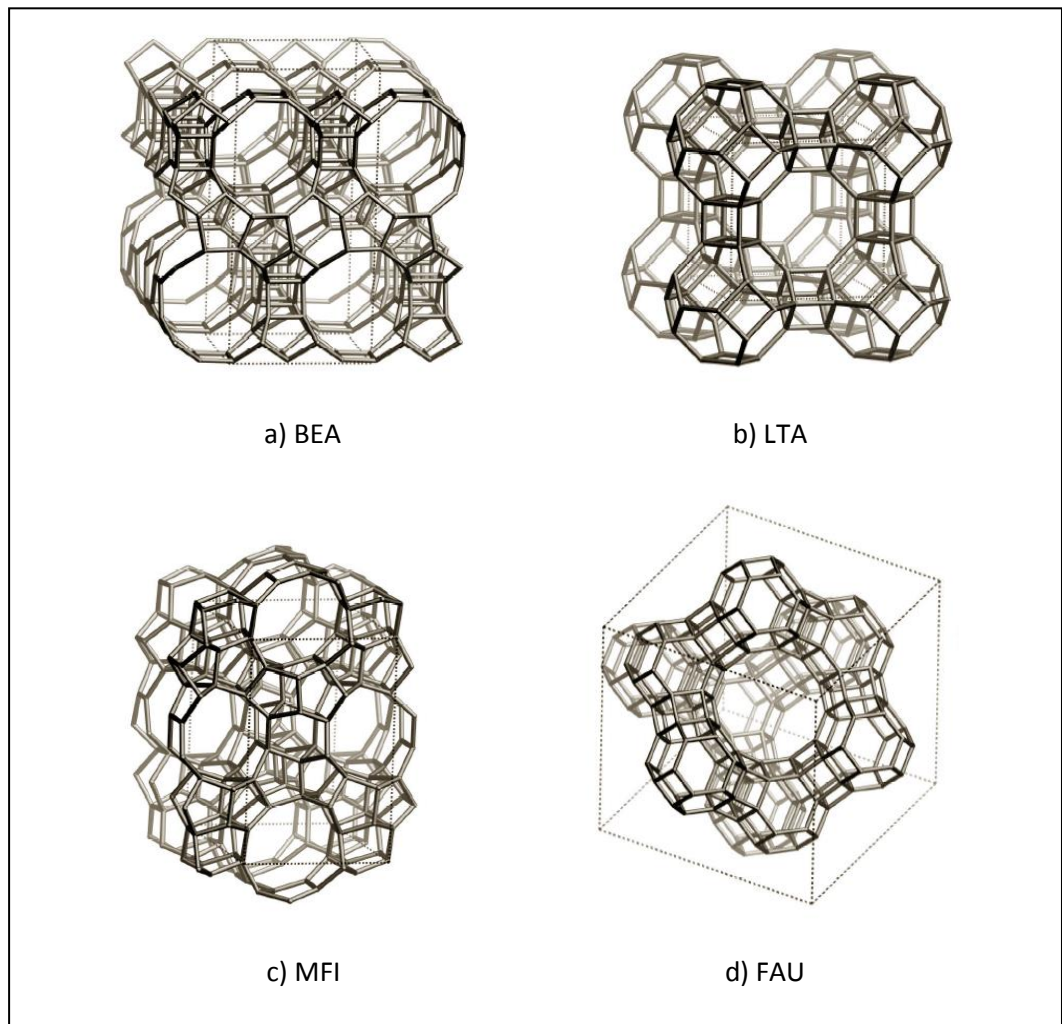


Figure 1.2. 3D structure of zeolite crystal a) zeolite beta (BEA), b) zeolite Linde type A (LTA), c) ZSM- 5 (MFI), d) zeolite Faujasite (FAU) (IZA, 2005)

Currently there are about 160 zeolites with different framework structure has been recorded in the Atlas of Zeolite Framework Types which can be accessed through the IZA website (<http://www.iza-structure.org>).

1.6 Nanocrystalline Zeolite

The crystal size of zeolites has a great influence on the catalytic activity and selectivity. In recent years, there has been a growing interest in the synthesis and application of nanosized zeolites. Nanocrystalline zeolite crystals have received considerable attention in the catalysis community and several research groups have devised synthesis conditions that yield small zeolite crystals (Jacobsen, 2000). Zeolites with a crystal size smaller than 100 nm are the potential replacement for existing zeolite catalysts (Larsen, 2007). The transition from micro to nanocrystallinity can be envisioned as the transition of extended symmetry of atoms of the crystal to just few unit cells (Singh *et al.* 2008). It is generally recognized that crystal sizes of zeolites have a significant influence in reactions involving the external surface and controlled by a diffusion process (Zhang *et al.* 2006). Selectivity to desired products also may be enhanced because unwanted by-product formation is less likely owing to better zeolite micropore utilization via shorter intracrystalline diffusion pathways, or simply because catalysts prepared from nano-zeolites may have more uniform active sites.

Singh *et al.* (2008) reported that there is an increased in ratio of atoms at or near the surface relative to the number of atoms on the inner part of the crystal. Ratio of external to internal number of atoms increases rapidly as the particle size decreases. The added advantage of nano-zeolite is that the smaller crystal of zeolite

has larger surface areas and less diffusion limitations compared with the zeolite of micrometer range (Lee *et al.* 2008).

The synthesis of nano-zeolite was reported by Verduijn and coworkers (1997). These syntheses produced colloidal sols of zeolites in uniform crystal sizes and have been developed for the preparation of zeolite films and membranes. Van Grieken *et al.* (2000) prepared ZSM-5 under hydrothermal conditions at autogenous pressure from clear supersaturated synthesis mixtures.

Willis and Benin (2007) reported that nano-zeolites are more active than typical one micron and larger zeolite crystals in heterogeneous catalysis applications. The amount of external acid sites of nanoscale HZSM-5 (70-100 nanometer) was 32 % of the total amount of acid sites, while that of microscale HZSM-5 (1-2 micrometer) was only 3 % (Zhang *et al.* 1999). The external surface acidity is a property of high relevance when the zeolite is intended to be used as a catalyst in reactions involving bulky molecules (not able to enter micropore system) such as polymer degradation and cracking of heavy oil fractions (Aguado *et al.* 2004). ZSM-5 zeolite with nanoscale crystal size has larger intercrystalline void space, larger pore volume, and more external surface acid sites, and it exhibits higher activity, lower coke content and better stability, which attracts a growing interest in the synthesis and application of nano-zeolites (Ding *et al.* 2007).

The reduction in the crystal size of zeolite Y resulted in an increased activity and selectivity in Fluidized Catalytic Cracking (FCC) due to improved diffusion of reactants and products. In catalytic cracking of vacuum gas oil using zeolite Y as the catalyst, smaller crystal sizes produced more gasoline and diesel, with less coke and gases (Jacobsen *et al.* 2000). Nanocrystalline Y zeolites may be particularly useful in

environmental applications as a NO_x storage-reduction (NSR) due to the small crystal size and large internal and external surface areas (Song *et al.* 2005).

1.7 Problem Statement

The production of biofuels such as diesel and gasoline fractions as an alternative fuel obtained from natural oils or fats has received much interest due to the depletion of fossil fuel, and also environmental concerns about global pollution. The direct conversion of edible palm oil to fuel may not be economically feasible because it can cause negative impact to the world, such as depletion of food supply leading to economic imbalance. One of the suitable ways to solve this problem is to utilize used cooking palm oil. In recent years, there has been a growing interest in the synthesis and application of nanocrystalline zeolites. Nano-crystal zeolites with a crystal size smaller than 100 nm are the potential replacement for existing zeolite catalysts due to its larger surface areas and less diffusion limitations compared with the zeolite of micrometer range. With decrease in crystal size, it is also important to investigate the physicochemical properties of nanocrystalline zeolite. Due to the current interest on such materials provide smaller crystal size, an opportunity for the development of more efficient cracking catalysts for the cracking of used cooking palm oil need to be explored. The optimum operating conditions for the production of liquid fuel are also essential in the study and can be obtained using statistical experimental design technique. Most of the reactions involving oil fractions, the catalyst deactivates by active site coverage due to coke formation, depending on the catalyst age. The catalyst decay phenomenon could be quantified using empirical functions of the time on stream. Based on the process studies for the cracking of used palm oil over nanocrystalline zeolite catalyst, a deactivation kinetic model and coke

combustion kinetic of catalyst after cracking reaction are needed for a better understanding of the process.

1.8 Objectives

1. To synthesize nanocrystalline zeolite ZSM-5, nanocrystalline zeolite Y and nanocrystalline zeolite beta.
2. To characterize the physico-chemical properties of synthesized nanocrystalline zeolites using different analytical techniques.
3. To study the catalytic activity of nanocrystalline zeolite ZSM-5, Y, and beta as cracking catalysts for the conversion of used palm oil and their selectivity for gasoline fraction production.
4. To determine the optimum operating conditions for biogasoline production over nanocrystalline zeolite as catalyst using design of experiments and response surface methodology.
5. To study the deactivation and coke combustion kinetics of the catalyst in used palm oil cracking reaction.

1.9 Scope of Study

This present study focussed on the synthesis of nanocrystalline ZSM-5, beta and Y zeolites using a clear solution method. The synthesized nanocrystalline zeolites were subjected to comprehensive characterization for changes in the characteristics of their structures using X-ray diffraction (XRD), Nitrogen adsorption-desorption isotherm, Scanning Electron Microscope (SEM), Transmission Electron Microscope (TEM), Fourier Transformed Infra Red Spectroscopy (FTIR),

Thermogravimetric Analyzer (TGA), and Temperature-Programmed Desorption (TPD) of NH₃.

The performance of nanocrystalline zeolites as catalyst was assessed in the cracking of used palm oil for the production of liquid fuel with interest in gasoline fraction. The catalytic properties of the catalyst were assessed in a microactivity testing (MAT) unit. The used palm oil (UPO) was used as the feedstock for the cracking activity of nanocrystalline zeolites in order to evaluate used palm oil as alternative source without competing with the edible oil market. The experiments were conducted at reaction temperature range of 400-500 °C, feed rate (WHSV) of 2.5 h⁻¹ and used palm oil to catalyst ratio range of 6-14. The optimum operating condition for maximum gasoline fraction yield was obtained from the statistical Design of Experiments (DoE) and response surface methodology (RSM). The effect of time on stream (TOS) on catalyst deactivation and deactivation parameters were obtained using different activity models. The coke combustion kinetics using thermogravimetric analysis (TGA) was studied for identification of different types of cokes responsible for deactivation and their regeneration temperatures were determined.

1.10 Organization of the thesis

This thesis was divided into five chapters:

Chapter 1: Introduction covers about the world's fuel demand and the importance of alternative fuels for transportation, the introduction of used palm oil as the potential source for the production of biofuel through catalytic cracking. A brief introduction about nanocrystalline zeolite is covered. The problem statement is included in this chapter for identification of the issues of the current research. The specific objectives

of the present study are presented leading to the solution of those issues. The scope of the study covers the research work done to cover these objectives.

Chapter 2: It provides literature review that covers information on the properties, synthesis, and application of zeolite as well as nanocrystalline zeolite, and also characterization of zeolite. Besides that, this chapter also reported literature covering catalytic cracking of vegetable oil mechanism and catalyst used. Finally, process studies and modeling of catalytic cracking process using statistical method, deactivation kinetics of cracking process and coke combustion kinetics are also covered.

Chapter 3: This chapter presents the experimental methodology and analysis. The details of the materials and chemical reagents used throughout this study are also presented. The procedures for catalyst preparation together with the characterization of the catalysts are also described. It also presents the used palm oil catalytic cracking reaction experimental setup, activity measurement of catalyst, products analysis, optimization study, deactivation study and coke combustion study.

Chapter 4: Results and discussion is divided into four sections: (a) nanocrystalline zeolite synthesis and characterization, (b) cracking activity of the synthesized zeolites as catalysts and (c) process optimization studies and (d) deactivation and coke combustion kinetics. The characteristic and the cracking activity of the synthesized zeolites as catalysts are presented and discussed. Statistical analysis and optimization based on Design of Experiments (DoE) and Response Surface Methodology (RSM) are covered. The deactivation of catalysts based on the time on

stream is presented. Deactivation model is proposed based on catalyst activity (φ) dependence on the time on stream (t) and deactivation rate parameter and order were estimated using non-linear regression analysis method based on Levenberg-Marquard's algorithm. Coke combustion kinetics using thermogravimetric method is also presented and activation energy for coke combustion was determined.

Chapter 5: Covers the summary and conclusions about the physicochemical properties of the synthesized catalysts, catalytic cracking activity, process studies parameter, modeling of cracking deactivation and coke combustion kinetics. The recommendations are also given in this chapter for the improvement of future research in this particular area.

CHAPTER 2

LITERATURE REVIEW

2.1 Zeolite

In 1756, the Swedish mineralogist A. F. Cronstedt heated an unidentified silicate mineral and observed that it fused readily in a blowpipe flame with marked expansion. These types of minerals were named ‘zeolites’ from the Greek words *zeo* (boil) and *lithos* (stone), because the rapid and unexpected departure of one of these guests (water) from a host (stilbite) on heating (Davis and Lobo, 1992). Since then, 48 naturally occurring zeolites have been discovered and more than 150 zeolite types have been synthesized.

The pore diameter of different zeolites depends on the number of tetrahedral in the ring around the pore with 8 tetrahedral as small-pore (0.4 nm), 10 tetrahedral as medium-pore (0.55 nm), 12 tetrahedral as large pore (0.8 nm) and more than 12 tetrahedral as ultra-large pore (1.8 nm) (Csicsery, 1995). International Union of Pure and Applied Chemistry (IUPAC) have classified the molecular sieve materials based on their pore size into three categories (Weitkamp *et al.* 1999):

- Microporous material pore diameter < 2.0 nm
- Mesoporous material $2.0 \text{ nm} \leq \text{pore diameter} \leq 50.0 \text{ nm}$
- Macroporous material pore diameter > 50.0 nm

Zeolites are microporous crystalline silicates and aluminosilicates linked through oxygen atoms, producing three-dimensional network channels and cavities of molecular dimension. The basic molecular structure of zeolite is shown in Figure

2.1. Zeolites have the chemical formula: $M_{2/n}O \cdot Al_2O_3 \cdot xSiO_2 \cdot yH_2O$

Where, the charge-balancing nonframework cation M has valence n , x is 2.0 or more, and y is the moles of water in the voids may vary from 2 to infinite. The value of x is equal to or greater than 2 because Al^{+3} does not occupy adjacent tetrahedral sites (Bhatia, 1990). Silicon and aluminium in aluminosilicate zeolites are referred to as the T-atoms (Weitkamp *et al.* 1999). The T-atoms are located at the vertices lines connecting them stand for T-O-T bonds. The primary building units are single TO_4 tetrahedra. Secondary building units (SBU), which contain up to 16 T-atoms, are derived from the assumption that the entire framework is made up of one type of SBU only. A unit cell always contains an integral number of SBU's.

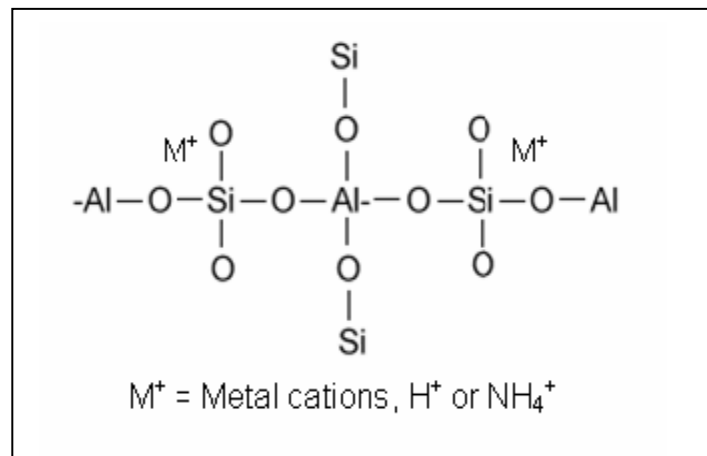


Figure 2.1. Zeolite basic unit structure (Guth and Kessler, 1999).

Structurally, the zeolite framework possesses a net negative charge which is balanced by the addition of protons (for instance, Na^+ , K^+ , or NH_4^+) due to zeolites comprise the assemblies of SiO_4 and AlO_4 tetrahedra joined together through the sharing of oxygen atoms with an open structure as shown in Figure 2.1. Many of these cations are mobile and can readily be exchanged with other ions in a contact solution. This ion-exchange property accounts for the greatest volume use of zeolites today.

Zeolites are also known as “molecular sieves” due to the well-defined pore structure. The term molecular sieve refers to a particular property of these materials,

i.e., the ability to selectively adsorb molecules based primarily on a size exclusion process. There are two types of phenomena in the molecular sieve which controls the reaction selectivity; either geometrically controlled (transition state selective) in zeolite or diffusion controlled (reactant or product selective) (Degnan, 2003). Product selectivity occurs when only products are small enough to leave through zeolites pores and larger product molecules may be formed or retained as intermediate within the zeolite cages.

The maximum size of the molecular or ionic species that can enter the pores of a zeolite is controlled by the diameter of the pore channels. Thus, the preliminary choice of a suitable zeolite for a specific reactant can be made based on the kinetic diameter of reactant. In general, zeolite pore sizes fall into the microporous size and with ring size between 8 – 20 (Guth and Kessler, 1999). The maximum size of the molecular or ionic species that can enter the pores of a zeolite is controlled by the diameters of the tunnels. These are conventionally defined by the ring size of the aperture, where the term "8 rings" refers to a closed loop that is built from 8 tetrahedrally coordinated silicon (or aluminium) atoms and 8 oxygen atoms. (Weitkamp *et al.* 1999).

The nomenclature associated with the zeolite was not uniform and hence International Zeolite Association (IZA) assigns three-letter code to the framework structure of each zeolite for instance FAU assigned for Faujasite. The designations to each framework are based on the connectivity of the tetrahedral atoms using the maximum topological symmetry, regardless of the changes in unit cell size and symmetry that may result from differences in chemical composition. These codes are particularly useful when there are many names for the same topology (there are 21 different names for molecular sieves with the MFI (Mobil number five: ZSM-5)

topology.). Therefore, we will use the most common name of the material and the three-letter code afterwards if considered necessary (Davis and Lobo, 1992). As illustrated in Figure 2.2 zeolites SOD, LTA, FAU, and are built by the same secondary building units (SBUs), sodalite cage, but via different connections. The supercage in FAU is surrounded by 10 sodalite units connected via the 6-rings by bridging oxygens. On the other hand, the 11.4Å cage in LTA is surrounded by eight sodalite units connected via the four-rings via bridging oxygens. NaY (FAU) is a large pore zeolite characterized by windows 7.4Å in diameter and tetrahedrally arranged about a 13Å diameter supercage.

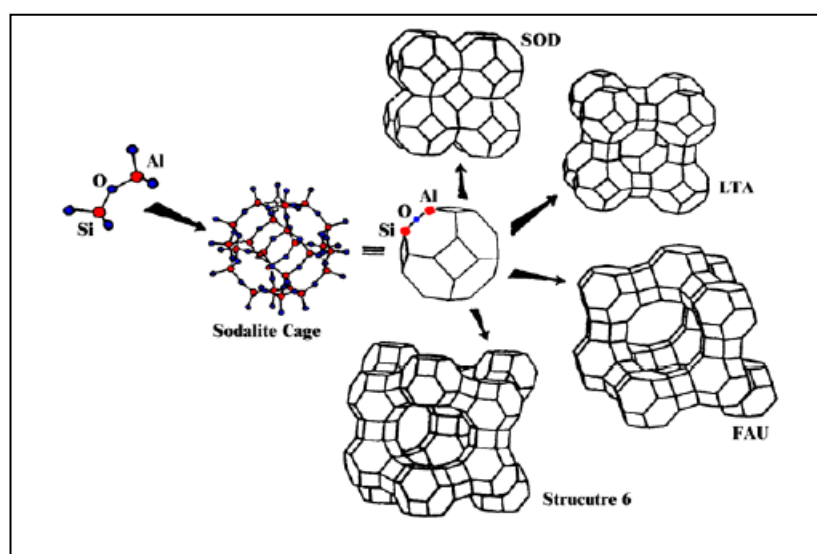


Figure 2.2. Schematic of Zeolite framework (Davis and Lobo, 1992)

2.1.1 Zeolite ZSM-5

ZSM-5 (Zeolite Socony Mobil) molecular sieve is a zeolite from the group of pentasil. The structure type code on zeolite nomenclature for ZSM-5 is MFI. ZSM-5, as synthesized, typically has a Si/Al ratio of 15, but it can be prepared with much higher ratios (up to thousands) to provide high temperature stability (Csicsery, 1995). ZSM-5 molecular sieve is a medium pore ($\sim 6\text{\AA}$) zeolite with three dimensional channels defined by 10-membered rings with two types of interconnected tubular and

circular type channels. The first of these pores is straight and elliptical in cross section (0.51×0.56 nm); the second pores intersect the straight pores at right angles, in a zig-zag pattern and are circular in cross section (0.54×0.56 nm) as shown in Figure 2.3 (Gates, 1992). The channel of ZSM-5 zeolite is short in length and large cavities present at the connection of the channels (Bhatia, 1990).

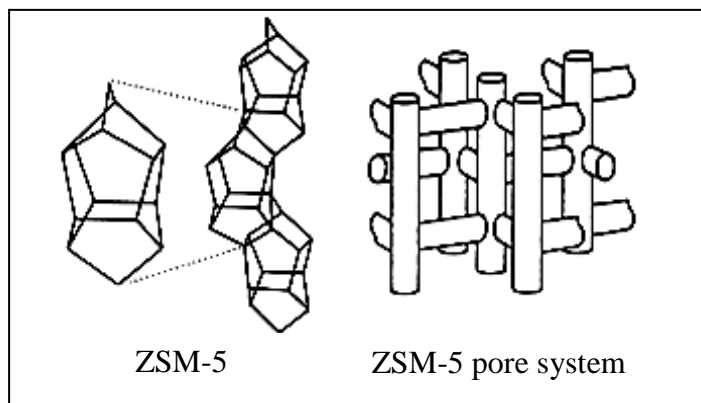


Figure 2.3. Framework structure of ZSM-5 (Gates, 1992).

In ZSM-5, the pore is of uniform dimension, the intersection provides an opening that can provide a type of cavity. The substitution of an aluminum ion (charge 3+) for a silicon ion (charge 4+) requires the additional existence of a proton, which gives the zeolite a high level of acidity, moreover causes its activity. ZSM-5 is usually synthesized in the presence of a tetra-alkyl ammonium cation or other organic compound as a template which is later, removed by calcinations (Davis and Lobo, 1992).

Since the discovery, ZSM-5 has been extensively utilized in industrial processes because of its outstanding catalytic properties and high thermal stability (Dwyer and Degnan, 1993). ZSM-5 with unique shape selective properties played an important role in enhancing quality of the gasoline by increasing the gasoline octane number by selectively cracking linear versus branched olefins in the gasoline range in gas oil cracking once it was used as an additive (Scherzer, 1990). This increase

was obtained at the expense of the total of gasoline and was accompanied by an increased yield of light olefins, especially propylene i.e. olefins with a carbon number of five and lowers (den Hollander *et al.* 2001). In addition, ZSM-5 exhibited remarkable resistance to coking since coke precursor cannot form in the pores of ZSM-5 and most of the coke deposited on the outer surface of the crystals (Csicsery, 1995; Thomas and Thomas, 1997). Other key industrial processes catalyzed by ZSM-5 include xylene isomerization, toluene disproportionation and MTG process (methanol to gasoline), by taking the advantages of the shape selective properties of ZSM-5 (Corma, 2003).

2.1.2 Zeolite Y

The combination of acidity, hydrothermal stability, and pore size made Zeolite Y supreme as the main active component of cracking catalysts. It is for this reason that the creation of mesopores during hydrothermal treatment and the use of small-crystallite-size Y zeolite show an improvement in gas oil cracking activity. Zeolite Y is structurally and topologically related to the faujasite type zeolite FAU. However, the 7.4-Å pore opening of zeolite Y prevents the cracking of larger molecules and it occurs on the external surface of the crystallites. The FAU structure (structure of zeolite Y) is made up of 6-6 SBUs. In addition, it is possible to consider the sodalite cage, a truncated octahedron that has eight hexagonal and six square faces, as basic structure of zeolite Y (Auerbach *et al.* 2003).

The FAU structure is formed when half of the octahedral faces are joined together to form hexagonal prisms. The spherical internal cavity generated when eight sodalite cages are joined is called the α -cage (or supercage) and is about 13 Å in diameter. Entry into the spherical α -cage can occur through four identical openings